



LAWRENCE
LIVERMORE
NATIONAL
LABORATORY

Surface-mediated suppression of radiation damage in GaN

S. Charnvanichborikarn, M. T. Myers, L. Shao, S. O. Kucheyev

November 15, 2011

Scripta Materialia

Disclaimer

This document was prepared as an account of work sponsored by an agency of the United States government. Neither the United States government nor Lawrence Livermore National Security, LLC, nor any of their employees makes any warranty, expressed or implied, or assumes any legal liability or responsibility for the accuracy, completeness, or usefulness of any information, apparatus, product, or process disclosed, or represents that its use would not infringe privately owned rights. Reference herein to any specific commercial product, process, or service by trade name, trademark, manufacturer, or otherwise does not necessarily constitute or imply its endorsement, recommendation, or favoring by the United States government or Lawrence Livermore National Security, LLC. The views and opinions of authors expressed herein do not necessarily state or reflect those of the United States government or Lawrence Livermore National Security, LLC, and shall not be used for advertising or product endorsement purposes.

Surface-mediated suppression of radiation damage in GaN

S. Charnvanichborikarn* and S. O. Kucheyev

Lawrence Livermore National Laboratory, Livermore, California 94550

M. T. Myers

*Lawrence Livermore National Laboratory, Livermore, California 94550 and
Department of Nuclear Engineering, Texas A&M University, College Station, Texas 77843*

L. Shao

*Department of Nuclear Engineering, Texas A&M University, College Station, Texas 77843
(Dated: October 25, 2011)*

Surfaces and interfaces are often sinks for radiation-generated mobile defects. This concept could be potentially used for designing materials with improved radiation resistance. However, in addition to promoting defect recombination, interfaces often cause detrimental disorder accumulation, particularly in non-metallic materials. Here, we demonstrate that the GaN surface is an efficient sink for mobile point defects, promoting their annihilation. We study structural damage in GaN bombarded at room temperature with 500 keV Xe ions at different incident angles in order to control the depth of the displacement generation profile without changing the average density of ballistic collision cascades. We find that, when point defects are generated within ~ 50 nm from the surface, they experience efficient recombination without any measurable increase in the rate of surface amorphization. As a result, the damage production efficiency is dramatically reduced within ~ 50 nm from the sample surface. Our findings provide clear experimental evidence of efficient suppression of radiation damage by an interface in a non-metallic material.

Radiation damage is a limiting factor for several technologies. These include ion implantation doping and etching of semiconductor devices, structural and fuel materials for nuclear power reactors, and electronics for use in a radiation environment. Minimizing undesirable radiation damage is a common challenge in all these fields. A strategy that has recently been pursued by a number of research groups for designing radiation-resistant materials is to maximize the number of interfaces such as free surfaces, grain boundaries, or interfaces between dissimilar materials. This strategy is based on a well known concept that interfaces are potential sinks for radiation-generated mobile defects and impurity atoms. If trapping of defects at interfaces leads to defect recombination, increasing the number of interfaces will improve radiation resistance. There is indeed some experimental evidence of an interface-mediated improvement of radiation resistance in several *metallic* systems. Examples include nanocrystalline metals (Pd,¹ Au,² Ni,³ Cu-0.5Al₂O₃,³ and TiNi^{4,5}) and oxide-dispersion strengthened (ODS) steels.⁶

Consequences of the interaction of radiation-generated mobile defects with interfaces, however, are presently not so optimistic for a large class of amorphizable *non-metallic* inorganic materials such as semiconductors and many ceramics. While interfaces could potentially promote defect recombination, as appears to be a case for some metals,¹⁻⁶ they could also act as the primary nucleation site for detrimental disorder accumulation, stoichiometric imbalance, and phase transformations. For example, the surface proximity in Si (arguably the most extensively studied non-metal) inhibits recombination of radiation-generated defects and, hence, severely deteriorates material's radiation resistance. Indeed, it has been known for a long time that the Si surface is a defect sink and a preferential nucleation site for amorphization.⁷⁻¹⁰ The fact that the Si surface also strongly inhibits defect recombi-

nation has recently been demonstrated by van den Berg and coworkers.^{11,12} A similar effect of a decreased radiation resistance has also been reported for Si,¹³ Ge,¹⁴ SiC,^{15,16} SnO₂,¹⁷ and ZrO₂ (Ref. 18) nanocrystalline materials.

An improved resistance to complete lattice amorphization has been reported for nanocrystalline forms of complex oxides, MgGa₂O₄ (Ref. 19) and Gd₂(Ti_{0.65}Zr_{0.35})₂O₇ (Ref. 20), with grain sizes of ~ 8 and ~ 20 nm, respectively. Subsequent study,²¹ however, pointed to a dominant role of stoichiometric disorder (rather defect recombination by an interface) in Gd₂(Ti_{0.65}Zr_{0.35})₂O₇ nanocrystals in determining their radiation resistance. Some mechanisms other than defect recombination at interfaces are also likely responsible for a high stability of MgGa₂O₄ nanocrystals to amorphization reported in Ref. 19 since, in the same report,¹⁹ the MgGa₂O₄ surface has been demonstrated to be a nucleation site for disorder accumulation.¹⁹ Hence, we must conclude that unambiguous experimental evidence of suppression of radiation damage by an interface in a non-metallic material is still to be demonstrated, while numerous recent reports have suggested adverse effects of interfaces in this class of materials.⁷⁻¹⁸

For another extensively studied non-metallic material, GaN, previous experiments have shown that the surface or the amorphous/crystalline (a/c) interface acts as a defect sink and is a nucleation site for amorphization.²² Bombardment results in layer-by-layer amorphization proceeding from the sample surface. A recent experimental study²³ has further revealed that the GaN surface, as compared to stable radiation damage in the crystal bulk, is a more efficient sink for mobile point defects with respect to both processes of point defect recombination and trapping. It is, however, not clear whether mobile defects trapped at the GaN surface experience annihilation or contribute to detrimental surface amorphization. In other words, does the GaN surface (or the a/c interface) im-

prove or deteriorate material's radiation resistance?

In this letter, we demonstrate that the GaN surface acts as an efficient sink for mobile defects, causing their *recombination*. Defects recombine at the surface without changing the rate of surface amorphization. To our knowledge, this is the first clear experimental demonstration of suppression of radiation-induced disorder by an interface in a non-metallic material. In addition to providing a strategy for minimizing radiation damage in GaN-based devices, our results have important implications to designing radiation-resistant materials.

About 2- μm -thick undoped wurtzite GaN (0001) epilayers, grown on *c*-plane sapphire substrates by metalorganic chemical vapor deposition, were used as irradiation targets. The 4 MV ion accelerator (National Electrostatics Corporation, model 4UH) at Lawrence Livermore National Laboratory was used for both ion irradiation and ion beam analysis. Implantation was done with 500 keV Xe ions to various fluences between 1×10^{14} and $2 \times 10^{15} \text{ cm}^{-2}$. During irradiation, the sample normal was tilted 7° , 60° , and 72° from the ion beam incidence direction. This was done in order to form near-surface damage layers with the same overall shape but with different thickness while maintaining a constant average density of collision cascades (which is known to influence radiation damage in GaN).²⁴ For a better comparison of data for different sample tilt angles, we express ion fluences in displacements per atom (DPA) at the depth of the maximum nuclear energy loss (R_{pd}). Quoted DPA values, calculated with the SRIM code (version SRIM-2008.04)²⁵ with effective threshold energies for atomic displacements of 25 eV for both Ga and N sublattices, are the concentrations of ion-beam-generated lattice vacancies at R_{pd} , normalized to the atomic concentration of GaN ($8.85 \times 10^{22} \text{ atoms cm}^{-3}$). During irradiation, beam flux values were kept constant to maintain a constant displacement generation rate of $\sim 7 \times 10^{-3}$ DPA/s at R_{pd} .

The damage buildup was measured by Rutherford backscattering/channeling (RBS/C) spectrometry with a 2 MeV $^4\text{He}^+$ beam incident along the [0001] channeling direction. A detector located at 103° from the incident beam direction was used to register backscattered particles, providing enhanced depth resolution. All RBS/C spectra were analyzed with one of the conventional algorithms²⁶ for extracting the effective number of scattering centers (referred to henceforth as “relative disorder”). Deconvolution by fitting disorder depth profiles with a bimodal Gaussian distribution was used to evaluate the thickness of surface amorphous layers (SALs).

Figure 1(a) shows SRIM-simulated depth profiles of lattice vacancies generated in GaN by Xe-irradiation at 7° , 60° , and 72° . These profiles are Gaussian-like (unimodal) with maxima at corresponding R_{pd} values that, as expected, get shallower with increasing sample tilt angle. Profiles of stable post-implantation lattice disorder measured by RBS/C are shown in Figs. 1(b) and 1(c) for ion fluences resulting in ~ 3 and ~ 6 DPA at R_{pd} , respectively. Such experimental profiles are bimodal, with a strong peak at the surface and a bulk defect peak (BDP), whose maximum (h^{max}) is deeper than R_{pd} . Both the bimodal nature of damage-depth profiles and a shift of h^{max} relative to R_{pd} are consistent with previous

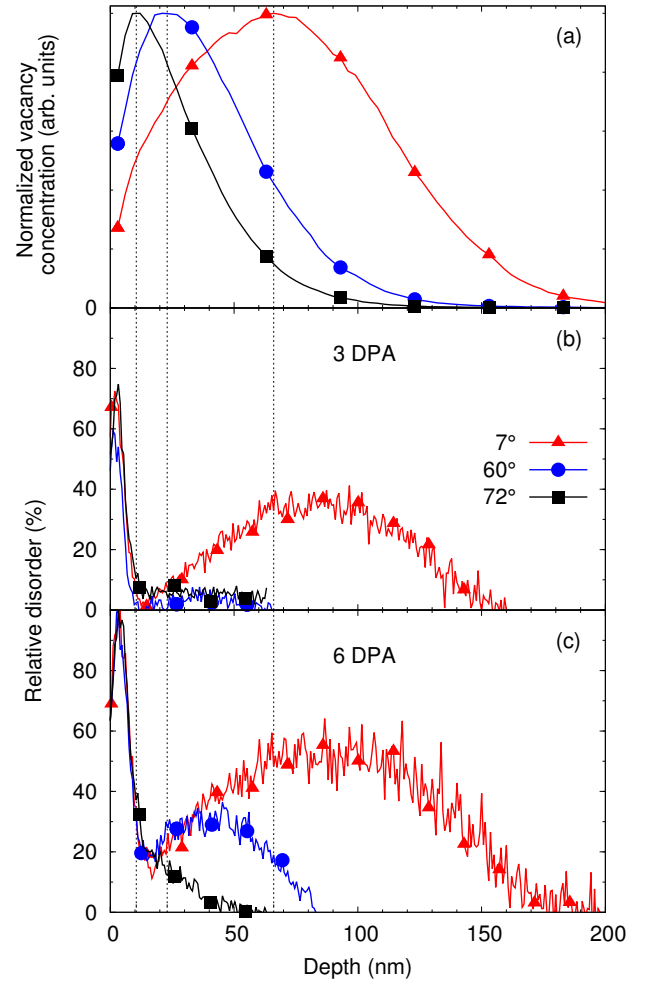


FIG. 1: (Color online) (a) Depth profiles of lattice vacancies ballistically generated in GaN by irradiation with 500 keV Xe ions with different incident beam angles relative to the sample surface normal (results of SRIM simulations). Positions of the maxima of such profiles are indicated by vertical dash lines. (b) and (c) Depth profiles of relative disorder for samples irradiated at various angles to fluences of ~ 3 and ~ 6 DPA, respectively. For clarity, only every 20-th experimental point is depicted.

observations.^{22,27–29} As discussed in detail elsewhere,^{22,23} for ion fluences above ~ 1 DPA, the surface defect peak originates from a SAL.

From a comparison of Figs. 1(b) and 1(c), it is seen that, for all tilt angles, an increase in ion fluence results in a corresponding increase in the BDP magnitude and the SAL thickness. More importantly, for both cases of ~ 3 and ~ 6 DPA, decreasing the depth of the displacement generation profile (by increasing the incident beam angle) dramatically reduces the BDP but has a negligible effect on the SAL thickness. The ion fluence dependence of the SAL thickness is plotted in Fig. 2(a) (the right axis). It illustrates that, with increasing fluence, the SAL grows at a constant rate of $\sim 0.75 \text{ nm/DPA}$,³⁰ independent of the proximity of the BDP to the a/c interface.

The fact that shallower implants result in lower bulk damage is better illustrated in Fig. 2(b), showing an ion fluence

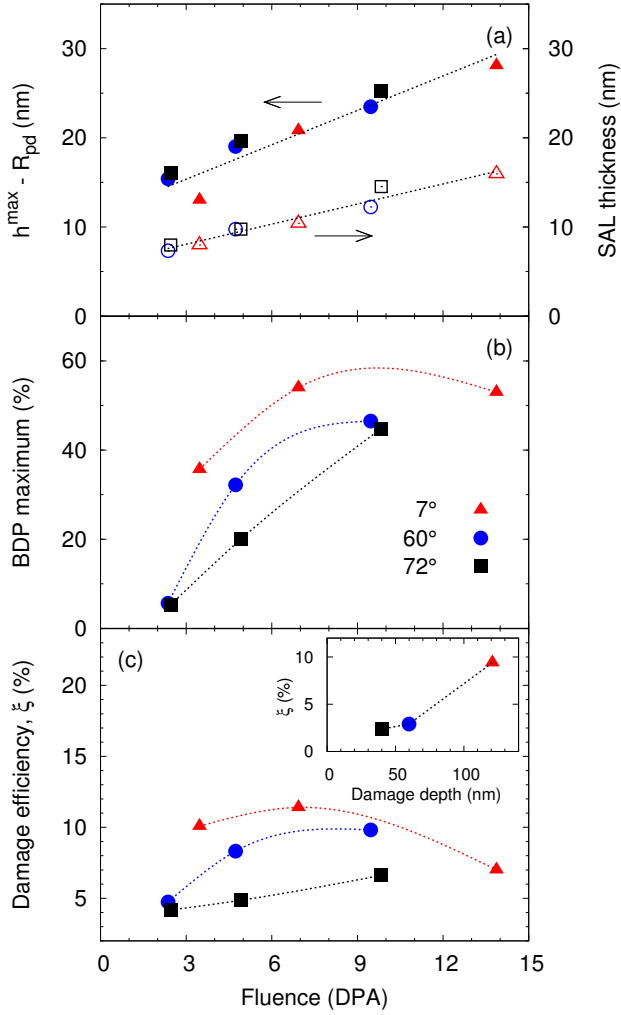


FIG. 2: (Color online) Ion fluence dependencies of (a) (left scale, closed symbols) the distance between the bulk defect peak (h^{\max}) and the maximum energy loss (R_{pd}) and (a) (right scale, open symbols) the thickness of surface amorphous layers for all three irradiation angles. (b) The bulk defect peak maximum and (c) the damage production efficiency as a function of fluence. The inset shows the damage production efficiency for the lowest fluence as a function of the damage generation depth, $R_{pd} + \Delta R_{pd}$. Dotted lines are guides to the eye. In all panels, the triangle, circle, and square symbols represent the data for 7°, 60°, and 72° angles, respectively.

dependence of the level of relative disorder at the BDP maximum. For all three sample tilt angles, with increasing fluence, the BDP level increases, approaching a saturation value of $\sim 50\%$. Such a saturation of the BDP maximum is consistent with previous reports.²²

The influence of the sample surface on defect recombination is further illustrated by Fig. 2(c). It shows a fluence dependence of the bulk damage production efficiency (ξ), which we define here as the ratio of depth-integrated stable bulk damage (without the contribution from the SAL) to the total number of vacancies (calculated by the SRIM code) bal-

listically generated by the ion beam in the region outside the SAL. As expected,^{22,24} $\xi \ll 100\%$, which means that post-irradiation damage is much lower than that predicted by ballistic collision cascade simulations. This is a consequence of very efficient dynamic annealing processes in GaN.

Figure 2(c) also shows that, for conventional irradiation at 7°, the ξ initially increases up to $\sim 10\%$ with increasing fluence and then decreases due to damage saturation in the BDP for fluences $\gtrsim 6$ DPA. Such a decrease in ξ indicates that elementary point defects generated in the BDP region in the saturation regime experience efficient recombination rather than migrating away from the BDP region and contributing to its expansion, as speculated earlier.³¹

The inset in Fig. 2(c) plots ξ for samples irradiated at different angles to ~ 3 DPA as a function of the damage generation depth, $R_{pd} + \Delta R_{pd}$, where ΔR_{pd} is a depth corresponding to one standard deviation of the Gaussian fit to SRIM-calculated displacement profiles. It is seen that the ξ rapidly increases when damage generation depth is larger than ~ 50 nm. Implants shallower than ~ 50 nm exhibit a decreased ξ , demonstrating an important role of the GaN surface in the elimination of mobile point defects.

Finally, Fig. 2(a) (the left axis) illustrates the effect of the BDP shift to larger depths with increasing ion fluence. Specifically, it shows a fluence dependence of the difference between the BDP position and R_{pd} for three tilt angles. It is seen that, for the fluence range studied, the BDP shift increases almost linearly with ion fluence. More importantly, the BDP shift is independent of R_{pd} : the BDP shifts a similar distance for a given fluence (expressed in DPAs) for all incident angles. Furthermore, Fig. 2(a) shows that the BDP shifts faster than the SAL growth rate. This behavior is in contradiction with a model³² recently proposed to explain the BDP shift in GaN. The main assumption of this model³² is that the BDP shift is caused by the proximity of the a/c interface, and, hence, different BDP shifts are expected for irradiation conditions with vastly different R_{pd} , as used in the present study. Since this is in contrast to observations summarized in Fig. 2(a), some mechanisms other than the interaction of mobile point defects with the sample surface or the a/c interface must be responsible for the BDP shift, and this intriguing effect deserves further studies.

In summary, the effect of the surface on radiation damage in GaN has been studied by varying the incident ion beam angle in order to control the depth of the profile of ion-beam-generated atomic displacements without changing the average density of ballistic collision cascades. Our observations indicate that the efficiency of the stable disorder formation is dramatically reduced for depths $\lesssim 50$ nm from the sample surface. This provides clear demonstration of the suppression of radiation damage by the GaN surface.

This work was performed under the auspices of the U.S. DOE by LLNL under Contract DE-AC52-07NA27344.

-
- * Electronic address: charnvanichb1@llnl.gov
- ¹ M. Rose, A. G. Balogh, and H. Hahn, Nucl. Instr. Methods Phys. Res. B **127/128**, 119 (1997).
 - ² Y. Chimi, A. Iwase, N. Ishikawa, M. Kobiyama, T. Inami, and S. Okuda, J. Nucl. Mater. **297**, 355 (2001).
 - ³ N. Nita, R. Schaeublin, M. Victoria, and R. Z. Valiev, Phil. Mag. **85**, 723 (2005).
 - ⁴ H. Wang, R. Araujo, J. G. Swadener, Y. Q. Wang, X. Zhang, E. G. Fu, and T. Cagin, Nucl. Instr. Methods Phys. Res. B **261**, 1162 (2007).
 - ⁵ A. R. Kilmametov, D. V. Gunderov, R. Z. Valiev, A. G. Balogh, and H. Hahn, Scripta Mater. **59**, 1027 (2008).
 - ⁶ See, for example, S. Ukai and M. Fujiwara, J. Nucl. Mater. **307–311**, 749 (2002).
 - ⁷ A. I. Gerasimov, E. I. Zorin, P. V. Pavlov, and D. I. Tetelbaum, Phys. Status Solidi A **12**, 679 (1972).
 - ⁸ V. N. Gashtold, N. N. Gerasimenko, A. V. Dvurechenskii, L. S. Smirnov, Sov. Phys. Semicond. **9**, 554 (1975).
 - ⁹ I. A. Abroyan, A. I. Titov, and A. V. Khlebalkin, Sov. Phys. Semicond. **11**, 712 (1977).
 - ¹⁰ H. A. Atwater and W. L. Brown, Appl. Phys. Lett. **56**, 30 (1990).
 - ¹¹ J. A. van den Berg, G. Carter, D. G. Armour, M. Werner, R. D. Goldberg, E. J. H. Collart, P. Bailey, and T. C. Q. Noakes, Appl. Phys. Lett. **85**, 3074 (2004).
 - ¹² J. A. van der Berg, M. A. Reading, D. G. Armour, G. Carter, P. C. Zalm, P. Bailey, and T. C. Q. Noakes, Rad. Eff. Def. Sol. **164**, 481 (2009).
 - ¹³ G. A. Kachurin, M. -O. Ruault, A. K. Gutakovsky, O. Kaïtasov, S. G. Yanovskaya, K. S. Zhuravlev, and H. Bernas, Nucl. Instr. Methods Phys. Res. B **147**, 356 (1999).
 - ¹⁴ M. C. Ridgeway, G. de M. Azevedo, R. G. Elliman, C. J. Glover, D. J. Llewellyn, R. Miller, W. Wesch, G. J. Foran, J. Hansen, and A. Nylandsted-Karsen, Phys. Rev. B **71**, 094107 (2005).
 - ¹⁵ W. Jiang, H. Wang, I. Kim, I. -T. Bae, G. Li, P. Nachimuthu, Z. Zhu, Y. Zhang, and W. J. Weber, Phys. Rev. B **80**, 161301 (2009).
 - ¹⁶ W. Jiang, H. Wang, I. Kim, Y. Zhang, and W. J. Weber, J. Mater. Res. **25**, 2341 (2010).
 - ¹⁷ P. K. Kuiri and J. Ghatak, Vacuum **85**, 135 (2010).
 - ¹⁸ A. Meldrum, L. A. Boatner, and R. C. Ewing, Phys. Rev. Lett. **88**, 025503 (2002).
 - ¹⁹ T. D. Shen, S. Feng, M. Tang, J. A. Valdez, Y. Wang, and K. E. Sickafus, Appl. Phys. Lett. **90**, 263115 (2007).
 - ²⁰ J. Zhang, J. Lian, A. F. Fuentes, F. Zhang, M. Lang, F. Lu, and R. C. Ewing, Appl. Phys. Lett. **94**, 243110 (2009).
 - ²¹ J. Zhang, J. Lian, F. Zhang, J. Wang, A. F. Fuentes, and R. C. Ewing, J. Phys. Chem. C **114**, 11810 (2010).
 - ²² See, for example, a review by S. O. Kucheyev, J. S. Williams, and S. J. Pearton, Mater. Sci. Eng., R **33**, 51 (2001); and references therein.
 - ²³ A. Yu. Azarov, A. I. Titov, and S. O. Kucheyev, J. Appl. Phys. **108**, 033505 (2010).
 - ²⁴ S. O. Kucheyev, A. Yu. Azarov, A. I. Titov, P. A. Karaseov, and T. M. Kuchumova, J. Phys. D: Appl. Phys. **42**, 085309 (2009).
 - ²⁵ J. P. Biersack, L. G. Haggmark, Nucl. Instr. Methods **174**, 257 (1980).
 - ²⁶ K. Schmid, Rad. Eff. **17**, 201 (1973).
 - ²⁷ S. O. Kucheyev, J. S. Williams, C. Jagadish, J. Zou, G. Li, and A. I. Titov, Phys. Rev. B **64**, 035202 (2001).
 - ²⁸ K. Lorenz, N. P. Barradas, E. Alves, I. S. Roqan, E. Nogales, R. W. Martin, K. P. O'Donnell, F. Gloux, and P. Ruterana, J. Phys. D: Appl. Phys. **42**, 165103 (2009).
 - ²⁹ W. Jiang, W. J. Weber, L. M. Wang, and K. Sun, Nucl. Instr. Methods Phys. Res. B **218**, 427 (2004).
 - ³⁰ This value of the SAL growth rate (~ 0.75 nm per DPA) is consistent with recent reports.^{23,24}
 - ³¹ S. O. Kucheyev, J. S. Williams, C. Jagadish, J. Zou, and G. Li, Phys. Rev. B **62**, 7510 (2000).
 - ³² A. I. Titov, P. A. Karaseov, A. Yu. Kataev, A. Yu. Azarov, and S. O. Kucheyev, Nucl. Instr. Methods Phys. Res. B (accepted).